MOLECULAR AND CELLULAR BIOLOGY, Feb. 2002, p. 1194–1202 Vol. 22, No. 4
0270-7306/02/$04.00+0 DOI: 10.1128/MCB.22.4.1194–1202.2002

Deletion of the Laminin α4 Chain Leads to Impaired Microvessel Maturation

Jill Thyboll,[1] Jarkko Kortesmaa,[1]† Renhai Cao,[2] Raija Soininen,[1]‡ Ling Wang,[1]§ Antti Iivanainen,[1]‖ Lydia Sorokin,[3] Mårten Risling,[4]# Yihai Cao,[2] and Karl Tryggvason[1]*

Division of Matrix Biology, Department of Medical Biochemistry and Biophysics,[1] Microbiology and Tumor Biology Center,[2] and Department of Neuroscience,[4] Karolinska Institutet, S-17 177 Stockholm, Sweden, and Interdisciplinary Center for Clinical Research, Nikolaus Fiebiger Center, 91045 Erlangen, Germany[3]

Received 31 August 2001/Returned for modification 26 October 2001/Accepted 19 November 2001

The laminin α4 chain, a component of laminin-8 and -9, is expressed in basement membranes, such as those beneath endothelia, the perineurium of peripheral nerves, and around developing muscle fibers. Laminin α4-null mice presented with hemorrhages during the embryonic and neonatal period and had extensive bleeding and deterioration of microvessel growth in experimental angiogenesis, as well as mild locomotion defects. Histological examination of newborn mice revealed delayed deposition of type IV collagen and nidogen into capillary basement membranes, and electron microscopy showed discontinuities in the lamina densa. The results demonstrate a central role for the laminin α4 chain in microvessel growth and, in the absence of other laminin α chains, in the composition of endothelial basement membranes.

Basement membranes (BMs) are thin extracellular sheet-like structures that compartmentalize tissues. By electron microscopy, they can be seen located beneath epithelia and endothelia as well as surrounding nerves, muscle fibers, and adipocytes. Most mature BMs contain laminin, type IV collagen, heparan sulfate core protein perlecan, and nidogen (entactin). Laminins are heterotrimeric multidomain glycoproteins composed of α, β, and γ chains. They are major structural elements of all BMs, but they also serve as signaling molecules through their interactions with cell surface receptors. In the BM, laminins are believed to exist as a polymerized two-dimensional network anchored on the cell surface via receptors, such as integrins, at the globular C-terminal domain of the α chain. In most mature BMs, type IV collagen is thought to form a more stable and rigid network, while nidogen is believed to serve as a bridge joining the independent networks of laminin and type IV collagen (4, 46). To date, five α, three β, and three γ chains have been identified (4), which exist in at least 12 heterotrimeric combinations (laminin isoforms 1 to 12) with different tissue distributions and functions. For instance, deficiency of the epithelium-specific laminin-5 (α3:β3:γ2) causes junctional epidermolysis bullosa (18, 35, 36), mutations in the α2 chain gene cause muscular dystrophy in both mice and humans (12, 47, 48), and lack of the widely expressed α5 chain in mice leads to multiple developmental defects, including exencephaly, syndactyly, and placental defects (28).

The laminin α4 chain (6, 13, 15, 27) is a component chain of laminin-8 (α4:β1:γ1) and laminin-9 (α4:β2:γ1) (29) and is widely distributed in vascular endothelial BMs of several tissues, as well as in BMs of the perineurium of peripheral nerves, heart, developing skeletal muscle, and developing kidney (6, 13, 23, 31). It has also been described in non-BM locations, e.g., in thrombocytes (7). The developmental expression patterns of the laminin α chains are complicated and not fully characterized in all tissues. In the capillaries of skeletal muscle, laminin α4 is first detected at embryonic day 11 (E11) and is retained at this site throughout development and into adulthood (13, 31). Laminin α5 is the other major laminin α chain known to occur in capillary BMs of muscle and most other tissues, but it appears later in development, at around 3 to 4 weeks postnatally (31, 43). One study recently reported that the laminin α2 chain was associated with capillaries in adult skeletal muscle (44), while an earlier study did not detect this chain in that particular location (31). Laminin α1 and α2 chains were previously reported as being expressed in the endothelial BMs of central nervous system capillaries (16, 34, 45), but it was recently shown that these chains are located in the parenchymal BM of the astrocyte endfeet surrounding these capillaries, and not in the endothelial BM (40). Since the laminin β2, β3, γ2, and γ3 chains have not been found in capillaries (14, 19, 31), laminin-8 is presumably the only laminin trimer in the capillary BMs of most embryonic and neonatal tissues.

The specific biological functions of laminin α4 and the isoforms containing this chain (laminin-8 and -9) are still poorly understood, and no human disease has been associated with absence or abnormalities in the laminin α4 chain. Its in vivo distribution provides some hints about possible functions. In particular, the widespread and exclusive expression of laminin α4 in basement membranes of developing microvessels suggests a role in angiogenic processes. We have previously shown

* Corresponding author. Mailing address: Division of Matrix Biology, Department of Medical Biochemistry and Biophysics, Karolinska Institutet, S-17 177 Stockholm, Sweden. Phone: 46-8-728 7720. Fax: 46-8-316 165. E-mail: Karl.Tryggvason@mbb.ki.se.

† Present address: BioStratum AB, SE-171 77 Stockholm, Sweden.

‡ Present address: Department of Medical Biochemistry, University of Oulu, FIN-90014 Finland.

§ Present address: The Burnham Institute, La Jolla, CA 92037.

‖ Present address: Faculty of Veterinary Medicine, University of Helsinki, FIN-00014 Finland.

Present address: The Swedish Defense Research Agency, S-172 24 Sundbyberg, Sweden.

that endothelial cells can bind laminin-8 through integrins α6β1 and α6β4 (20), and it is likely that laminin-8 interacts with the type IV collagen network of capillary BMs via nidogen, because it has a nidogen-binding site in its γ1 chain (9, 33).

In the present work, we have generated mice harboring *Lama4*-null alleles by gene targeting in embryonic stem (ES) cells. Newborn laminin α4-deficient mice exhibited hemorrhages in subcutaneous tissues and muscle with consequent anemia and restoration of an apparently normal phenotype during neonatal life. In adult null mice, the formation of blood vessels was dramatically affected in the cornea angiogenesis model, resulting in extensive bleeding and disorganization of microvessel growth. The results demonstrate that the laminin α4 chain has a significant role in the formation and structural integrity of newly formed capillary BMs.

MATERIALS AND METHODS

Targeting vector construction. Three overlapping lambda phage clones containing the first two exons of the *Lama4* gene were isolated from a murine 129Sv genomic library and characterized by restriction mapping. A 4-kb *Hin*dIII-*Bam*HI fragment containing the promoter and exons 1 and 2 was replaced with the PGK *Neo* cassette. For the short arm of the targeting construct, a 1.9-kb *Bam*HI-*Kpn*I fragment downstream of exon 1 was cloned into pSL 1180 vector (Pharmacia). The short arm fragment was excised with *Bam*HI and ligated to the *Bam*HI site of the plasmid containing the PGK *Neo* cassette. The long arm, the 5-kb *Hin*dIII fragment upstream of exon 1, was then ligated to the *Hin*dIII site. Finally, the blunt-ended herpes simplex virus-thymidine kinase (HSV-TK) cassette was ligated to the *Eco*RV site in the targeting vector.

Generation of *Lama4*$^{-/-}$ mice. ES cells (RW4; Genome Systems) were grown on an embryonic fibroblast layer as recommended by the supplier. The cells were electroporated with *Not*I-linearized targeting vector. Selection with G418 and ganciclovir was initiated 24 h after electroporation and continued for 6 to 8 days. Colonies with the targeted mutation were identified by PCR and Southern blot analysis. Cells from these colonies were injected into C57BL/6 blastocysts, which were transferred into pseudopregnant foster mothers. Highly chimeric males were mated with C57BL/6 females, and heterozygous offspring were interbred to obtain homozygous mutant mice or mated with wild-type C57BL/6 mice (Charles River Laboratories) for backcrossing.

Genotyping of ES cells and mice. Genomic DNA from ES cells or mouse tails was digested with *Eco*RI, separated on a 0.7% agarose gel, blotted to a nylon membrane, and hybridized with the labeled 300-bp fragment probe downstream of the targeting construct region. The probe hybridizes to a 9-kb wild-type fragment and to a 3-kb fragment in the targeted allele. Alternatively, a pair of PCRs with primers specific for the targeted allele (5′ TAA CTC ATA GCC ACT CTT ACA GAG C 3′ in *Lama4* intron 2 and 5′ GCT AAA GCG CAT GCT CCA GAC TG 3′ within the PGK promoter) and the wild-type allele (5′ GGC AGG CGT CCC AGT GTC 3′ in *Lama4* exon 1 and 5′ CAA CAA AGT TGC AAC TTG GGC TC 3′ in *Lama4* exon 2) were used to determine the genotype.

Northern blot analysis. Mouse heart, skeletal muscle, and lung tissues were dissected and immediately frozen in liquid nitrogen. Total or poly(A)-enriched RNA samples from normal and null mutant mice were separated side by side on a formaldehyde agarose gel and blotted by standard techniques to Biodyne B (Pall) charged nylon membranes. Blots were hybridized with random-primed, ^{32}P-labeled mouse cDNA probes for laminin α1, α2, α3, α4, and α5 chains. Laminin β1, perlecan, and GAPDH probes were used as internal controls to check RNA integrity and compensate for inequalities in loading. Radioactivity was detected and quantitated with PhosphorImager SI (Molecular Dynamics) and ImageQuaNT software.

Clinical chemistry. Hemoglobin was measured in whole-blood samples of newborn mice with a hemoglobin meter (HemoCue AB). It was necessary to pool blood from several newborn pups for automated blood analyses, because the volume of blood obtained from a single pup was insufficient for such analyses. Offspring from either +/+ or −/− parents were used for these analyses. Sampling was done immediately after decapitation with heparinized 75-μl glass capillaries (Kebo), and the blood was pooled into plastic EDTA-treated tubes (Becton Dickinson). About 25 to 50 μl of whole blood was obtained from one pup. Samples from adult mice were taken from the tail artery directly into EDTA-treated plastic tubes. The whole-blood analyses were performed with an ADVIA 120 analyzer (Bayer), except for reticulocytes, which were counted manually. For serum analyses, blood was collected and allowed to coagulate in 1.5-ml plastic tubes, which were then centrifuged at 2,500 × *g* for 12 min. Serum analyses were performed with a Vitrof 950 analyzer (Johnson & Johnson).

For activated partial thromboplastin time (aPTT) and prothrombin time (PT) analyses, blood was obtained from the heart into a syringe containing 0.1 M sodium citrate (1 part plus 9 parts of blood), transferred to a 1.5-ml tube with immediate mixing, and centrifuged for plasma separation. aPTT was determined on an ST2 clotting timer (Diagnostica Stago) by using Céphalite reagent (bioMérieux SA) according to the manufacturer's instructions with the modification that only 50 μl of plasma was used and the incubation time was 6 min. PT was determined by using the same equipment with Normotest reagent (Axis-Shield PoC AS) according to the manufacturer's instructions. Bleeding time was determined by cutting the tail 5 mm from the tip in mice anesthesized with isoflurane. Excess blood was wiped away every 30 s without dislodging the forming clot. Student's two-tailed *t* test was used for statistical analysis.

Histochemical analyses. Tissue samples were placed in a cryoprotectant medium, TissueTek (Sakura), in plastic molds and frozen in isopentane cooled to the freezing point. Cryosections 8 to 12 μm in thickness were made, and the sections were allowed to dry for 1 h at room temperature and then fixed in acetone for 10 min before staining, except for antibody S8, for which the sections were additionally treated for 5 min in boiling 1 M urea and washed in distilled water.

The antibodies used were anti-CD-31 (PECAM-1, clone MEC 13.3; PharMingen International), anti-nidogen or -entactin (monoclonal antibody [MAb] 1946; Chemicon), anti-collagen type IV (polyclonal antibody AB756P; Chemicon), anti-perlecan (clone HK-102; Seikagaku Corp.), anti-laminin α1 (clone 198 [42]), anti-laminin α2 (clone 4H8-2 [39]), anti-laminin α3 (clone D3-4 [10]), anti-laminin α4 (polyclonal S8 [13] and 341 [37]), anti-laminin α5 (4G6 and serum 405 [43]), anti-laminin β1 (clone LT3; Neomarkers, Inc.), and anti-laminin γ1 (clone 4C12; Immunotech [8]). Secondary antibodies were fluorescein isothiocyanate (FITC) or Cy3 conjugated and purchased from Jackson ImmunoResearch Laboratories, Inc. Tissue sections were examined with a Leica MDRB microscope, and pictures were taken with a Hamamatsu digital camera with Openlab (Improvision) software. Digital images were further processed with Photoshop 5.0 (Adobe).

For histochemical staining (hematoxylin and eosin, Maisson trichrome), the tissue samples were fixed in 4% paraformaldehyde or Histofix (Histolab), paraffin embedded, and stained according to standard protocols. Tissue sections were examined with a Leica MDLB microscope (Leica), and pictures were taken with a Nikon Coolpix 950 digital camera (Nikon). Digital images were further processed with Photoshop 5.0 (Adobe).

Electron microscopy. For electron microscopy, the specimens were fixed in 2% glutaraldehyde in phosphate buffer, osmicated, dehydrated in graded steps of acetone, and embedded in Vestopal W. Thin transverse sections were collected on 640-hex mesh grids, contrasted with uranyl acetate and lead citrate, and examined in a Philips EM201 electron microscope operated at 80 kV. Micrographs were scanned and processed with Photoshop 5.0 (Adobe).

Cornea angiogenesis assay. The mouse corneal assay was performed as previously described (2, 3). Briefly, corneal micropockets were created with a modified von Graefe cataract knife in the right eye of adult *Lama4*$^{-/-}$ mice and wild-type littermates. A micropellet (0.35 by 0.35 mm) of sucrose aluminum sulfate coated with Hydron polymer type NCC (IFN Sciences) containing 80 ng of human fibroblast growth factor 2 (FGF-2) was implanted into each pocket. The pellet was positioned approximately 1.2 mm from the corneal limbus. After implantation, erythromycin or ophthalmic ointment was applied to each eye. The corneal neovascularization was examined with a slit-lamp biomicroscope.

RESULTS

Generation of laminin α4-null mice. The *Lama4* gene was disrupted by homologous recombination as depicted in Fig. 1A, and two mouse lines originating from different ES cell clones were generated. Interbreeding of the heterozygote mice from both lines yielded wild-type, heterozygous, and homozygous offspring (Fig. 1B) at approximately Mendelian ratios of 1:2:1 (Table 1). Northern blot analyses demonstrated a complete absence of laminin α4 chain mRNA in null mice (Fig. 1C), and immunostaining of tissues confirmed the absence of

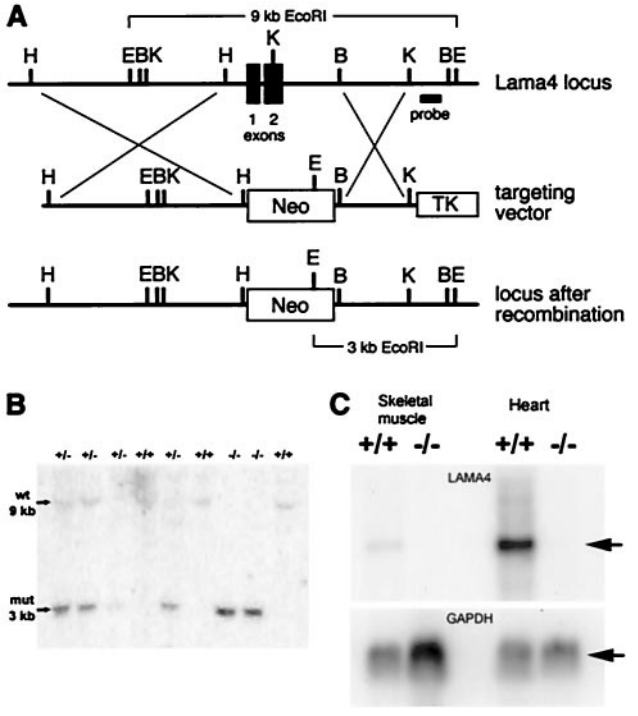

FIG. 1. Generation of laminin α4-deficient mice. (A) Targeted inactivation of the *Lama4* gene. The 5′ region of the *Lama4* gene (top), targeting vector (middle), and the gene region after homologous recombination (bottom). Exons depicted as black boxes are numbered. The probe used for the Southern blot is indicated (thick bar). (B) Southern blot analysis of *Eco*RI-digested genomic DNAs from a litter obtained by F_1 heterozygote mating. As depicted in panel A above, the wild-type (wt)-specific fragment is 9 kb, and the mutant (mut) fragment is 3 kb. (C) Northern blot analysis of RNA isolated from wild-type and null mouse muscle and heart. The filter was hybridized with a laminin α4 chain cDNA probe comprising nucleotides 1380 to 2596, and a GAPDH probe was used as an internal control for RNA loading and integrity.

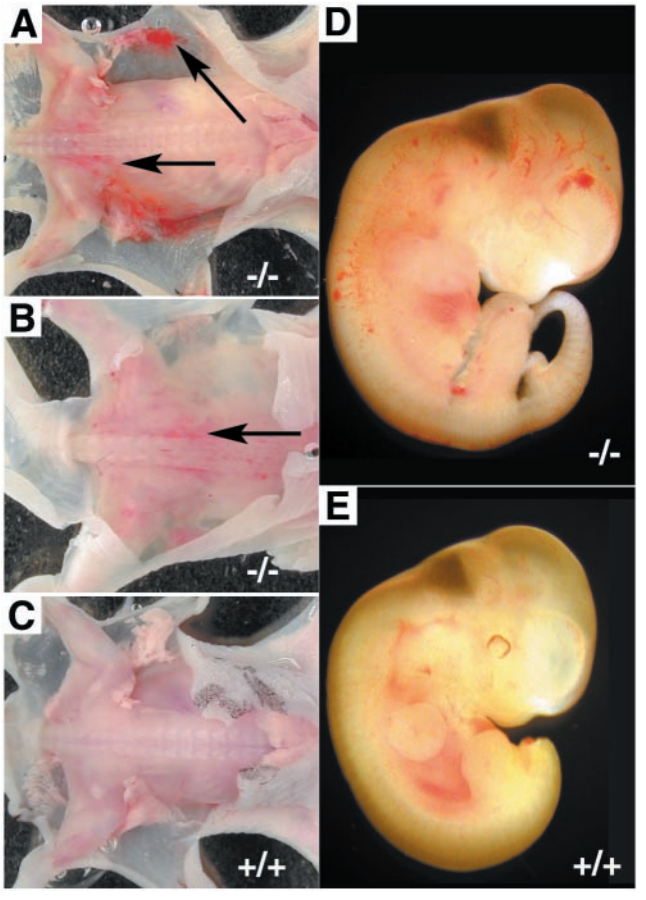

FIG. 2. Hemorrhages in the *Lama4*$^{-/-}$ mice. Following removal of the skin, hemorrhages were clearly seen in the subcutaneous fat and intramuscularly along the vertebral column (arrows) in the newborn −/− animal (A) and, to a lesser extent, in embryos at E18.5 (B), while no hemorrhages were seen in control newborns (C). Macroscopic bleeding could also be observed in −/− embryos at E11.5 (D), while littermate controls were normal (E).

the laminin α4 polypeptide (see Fig. 3K and L). The analyses described below were made with mice backcrossed for 7 to 10 generations in the C57BL/6 background and mice with a mixed 129Sv × C57BL/6 background.

During the first 2 days of postnatal development, the mortality of −/− mice was slightly elevated, and the pups were about 10% smaller than their wild-type littermates (Table 1). Null mice surviving beyond the perinatal period had mortality rates and life spans similar to those of their wild-type littermates (not shown). The adult null mice also frequently suffered from a mild motor impairment, which may be related to the abnormal development of the neuromuscular junction (30).

TABLE 1. Characteristics of newborn pups after interbreeding of *Lama4*$^{+/-}$ mice

Mouse type	% Genotype ratio at P0[a]	% Mortality at P0–P2	Birth wt ± SE (g)
+/+	28 (86/302)	<1 (0/76)	1.64 ± 0.04
+/−	49 (148/302)	<1 (1/134)	1.64 ± 0.03
−/−	23 (68/302)	6 (3/54)	1.49 ± 0.03

[a] P0, postnatal day 0.

This phenotype included uncoordinated movements of the hind limbs when suspended by the tail, and the mice slipped more often in a beam-walking test.

Hemorrhages and anemia in newborns. Newborn *Lama4*-null mice were lethargic, pale, and yellowish (icteric), and had diffuse subcutaneous hemorrhages in the soft tissues of the hind limbs, head, lower back, and neck regions (Fig. 2A). Mild hemorrhages were also seen in the heart and meninges, and, occasionally, blood was seen in the colorectum or intraperitoneally (not shown). In embryos just before birth (E18.5), significantly milder hemorrhages were frequently seen, especially along the vertebral column in the lower back (Fig. 2B). Hemorrhages had been seen already at E11.5 in about 50% (6 of 11 −/− and 0 of 22 littermate controls) of mutant embryos, particularly in the head (Fig. 2D). Macroscopically, the bleeding was restricted to smaller vessels, while larger vessels appeared to be unaffected. The hemorrhagic phenotype was observed in all newborn −/− pups, including those with the hybrid genetic background, but the severity varied. Hemorrhages were not seen in wild-type (Fig. 2C and E) or heterozygote (not shown) littermate embryos or newborns. Histological analyses of new-

TABLE 2. Clinical chemical analyses of newborn *Lama4*$^{-/-}$ and *Lama4*$^{+/+}$ mice[a]

Analyses	Result for mice:	
	−/−	+/+
Whole blood (*n*)	(6, 7)	(9, 8)
Hemoglobin (g/liter)	58, 59	129, 132
Hematocrit (%)	18, 20	38, 42
Erythrocyte count (10^{12} cells/liter)	1.8, 1.9	4.0, 4.3
Mean cell vol (fl)	100, 105	96, 98
Mean cell hemoglobin concn (g/liter)	288, 316	312, 329
Leukocyte count (10^9 cells/liter)	4.1, 4.7	3.2, 4.7
Platelet count (10^9 cells/liter)	228, 246	420, 492
Reticulocytes (% of erythrocyte count)	18, 19	10, 11
Serum (*n*)	(8)	(14, 8)
Albumin (g/liter)	10.9	10.5, 10.8
Unconjugated bilirubin (μmol/liter)	29.7	8.2, 8.8
Conjugated bilirubin (μmol/liter)	3.7	0.2, 1.2
Alanine aminotransferase (μkat/liter)	0.57	0.57, 0.66

[a] The values represent the results obtained from one or two pools of blood, where *n* indicates the number of animals in each pool.

born −/− mice revealed extravasal location of erythrocyte corpuscles (e.g., in loose connective tissues, striated muscle, and perineurally), while corresponding tissues in control littermates were unaffected (not shown).

Whole-blood analyses were carried out to examine if the paleness of newborn mice was due to anemia as a result of internal bleeding. These analyses revealed a drastic reduction in hemoglobin to 59 g/liter in −/− mice, as opposed to 130 g/liter in wild-type mice (Table 2). Accordingly, hematocrit and erythrocyte counts were significantly decreased in the −/− mice, while erythrocyte indices (mean cell hemoglobin and mean cell volume) were not significantly changed (Table 2). An increase in unconjugated bilirubin indicated excessive destruction of erythrocytes, and elevated relative reticulocyte counts suggested adequate erythrocyte formation. The platelet and leukocyte counts were not significantly different from those of the wild-type mice, and levels of albumin and alanine aminotransferase in serum were normal. The overall blood findings are consistent with anemia caused by internal bleeding. The hemorrhages disappeared in −/− mice a few days after birth, and the anemia normalized in newborn −/− mice within 2 weeks of postnatal life.

The bleeding of −/− mice after tail cutting for genotyping was not excessive, which indicated that blood coagulation was normal. In order to further examine potential blood coagulation abnormalities, we determined the aPTT, PT, and bleeding time. Adult animals were used, since there is a high risk of contaminating the sample with tissue proteins that affect coagulation assays when taking blood samples from newborns after decapitation. aPTT (time ± standard error, 31.7 ± 4.8 s [$n = 7$] in mutants versus 33.6 ± 1.8 s [$n = 4$] in controls), PT (37.9 ± 3.2 s [$n = 7$] in mutants versus 35.3 ± 1.3 s [$n = 4$] in controls), and bleeding time (233 ± 50 s [$n = 4$] in mutants versus 173 ± 51 s [$n = 4$] in controls) were measured, but none of the differences were statistically significant (all P values above 0.1).

Abnormal composition and structure of capillary BMs. Considering the expression pattern of laminin α4 in developing capillaries, the bleedings could be associated with structural abnormalities in capillary BMs. To study this, immunostainings were performed on newborn lower back muscle with antibodies against various BM components. Immunostaining with MAbs against the endothelial marker PECAM-1 (CD31) revealed no apparent changes in capillary density between wild-type and null mice (Fig. 3A and B). Interestingly, staining with antibodies detecting type IV collagen (Fig. 3C and D), nidogen (Fig. 3E and F), laminin β1 chain (Fig. 3G and H), and laminin γ1 chain (not shown) showed these proteins to be drastically reduced or in some cases practically absent in the capillaries of null mice, while they were present in normal amounts in the BMs surrounding the neighboring individual muscle fibers. In contrast, perlecan was deposited in the null mice as in wild-type littermates (Fig. 3I and J), and integrin α6 expression was unaffected (not shown). Thus, the absence of the laminin-8 isoform normally present in developing capillaries was accompanied by a reduction of type IV collagen and nidogen. In adult null mice, immunostaining of the BM components in muscle capillaries and muscle fibers was identical to that of controls, with the exception of laminin α4: Adult capillary BMs contained type IV collagen, laminin-10, nidogen, and perlecan, and the muscle fibers stained for type IV collagen and laminin-2, as well as for nidogen and perlecan (not shown).

Immunostaining further revealed that the laminin α1, α2, α3, and α5 chains were not present in the muscle capillaries of newborn null mice (Fig. 4). Furthermore, no upregulation of α1, α2, α3, or α5 genes was apparent by Northern blot analysis of RNA isolated from adult skeletal muscle, heart, or lung of −/− mice (not shown). Hence, the absence of laminin α4 was not compensated for by other laminin α chains, either in newborn muscle or in the adult tissues studied.

The staining pattern observed for BM proteins suggested structural abnormalities in the muscle capillaries of newborn laminin α4-deficient mice. Therefore, electron microscopic analyses were carried out on the capillary walls of the striated muscle of the lower back, which regularly showed extensive bleeding. The results showed that in the *Lama4*$^{-/-}$ mice, the lamina densa of the capillary BM was generally discontinuous, compared to the well-structured and more continuous lining in the control mice (Fig. 5). Other BMs, such as those of muscle fibers, appeared normal in −/− mice (not shown). In the adult muscle, the electron microscopic analysis revealed endothelial BMs that appeared normal (not shown).

Impaired blood vessel maturation. The transient defects observed in capillary BMs of newborn *Lama4*-null mice suggested that the laminin α4 chain plays a role in the formation of new microvessels. Therefore, we decided to examine whether the formation of new capillaries was also affected in adult *Lama4*-null mice. In the cornea angiogenesis assay (17), earlier and more intense sprouting of blood vessels was observed in *Lama4*$^{-/-}$ mice than in controls, after implantation of the FGF-2-containing pellet. At 3 to 5 days after insertion of the pellet, grossly distorted blood vessel architecture with hemorrhages (Fig. 6A to F) and dilated vessels (Fig. 7) could be seen. The branching pattern of blood vessels appeared irregular and uncoordinated. In about half of the cases, the bleeding and consequent swelling were so intense (Fig. 6F) that the animals had to be sacrificed. Immunofluorescent staining

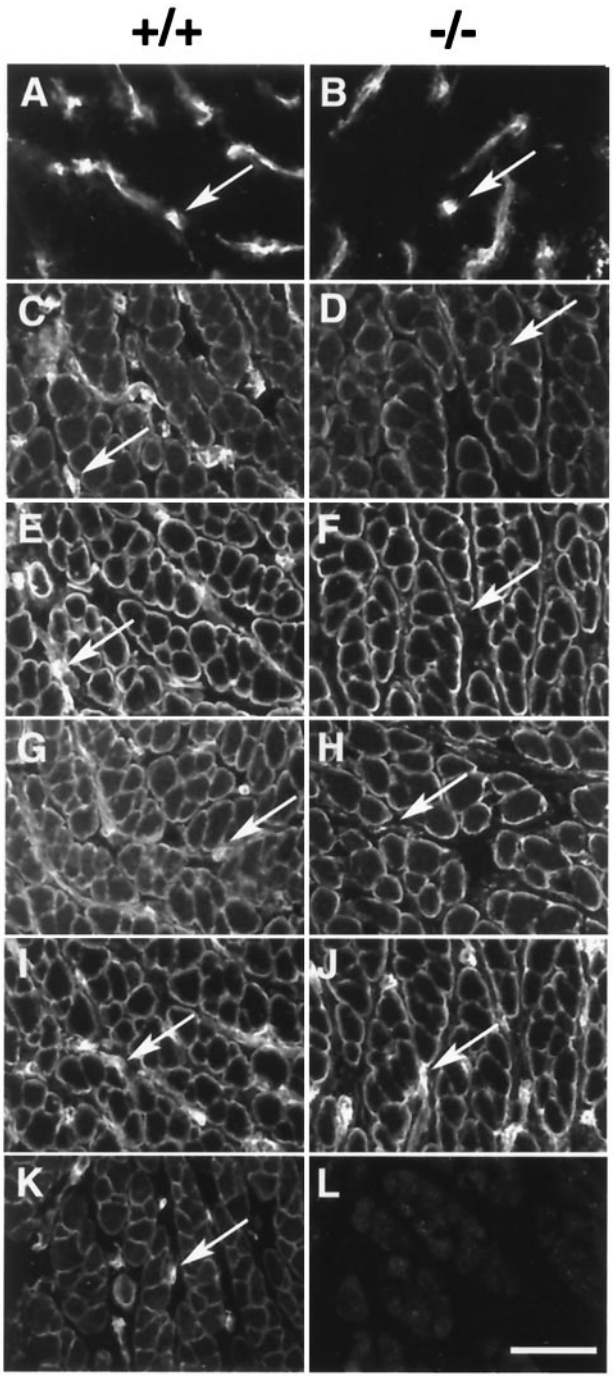

FIG. 3. Abnormal composition of the capillary BMs. Immunostaining of sections through muscles of the lower back of newborn *Lama4*$^{+/+}$ and *Lama4*$^{-/-}$ mice. Blood vessels were visualized with an antibody to the endothelium-specific protein PECAM-1 (A and B). Arrows indicate examples of cross-sectioned capillaries. The staining intensity in blood vessels of the mutants was drastically reduced with antibodies against type IV collagen (C and D). Similar results were obtained with antibodies to nidogen (E and F) and to the laminin β1 chain (G and H). Note that anti-type IV collagen, anti-nidogen, and anti-laminin-β1 antibodies all readily stained BMs surrounding individual muscle fibers of *Lama4*$^{-/-}$ mice and BMs of blood vessels of *Lama4*$^{+/+}$ mice. In contrast, perlecan could be seen in both capillary and muscle BMs in both −/− and +/+ mice (I and J). The laminin α4 chain is present around capillaries in the control mice (K), but it is totally absent in the mutant mice (L). Bar, 50 μm.

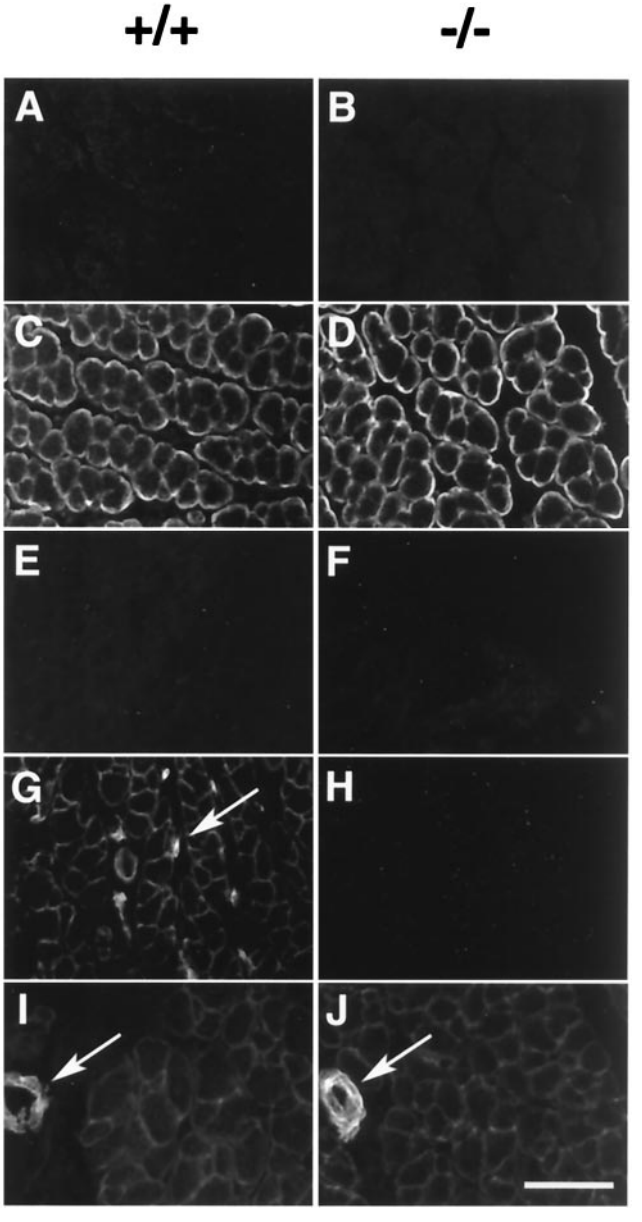

FIG. 4. Laminin α chains in newborn skeletal muscle. No α1 staining could be detected in either genotype (A and B). Laminin α2 was present around muscle fibers (C and D), but no staining was seen around capillaries. Laminin α3 was totally absent from newborn muscle (E and F). The α4 chain was present around capillaries in +/+ mice (G, arrow), but absent in −/− mice (H). Larger vessels were strongly stained for laminin α5 (I and J, indicated by arrows) and faintly stained for α4 (not shown). Around muscle fibers, faint staining was also seen with antibodies against the α4 and α5 chains. No difference was observed in the staining patterns of mutant mice, except for the absence of α4 (H). Bar, 50 μm.

showed that the laminin α4 chain was present in the newly formed vessels of wild-type animals (not shown). Faint staining was seen in a subset of blood vessels with an antibody to the laminin α5 chain 5 days after implantation of the pellet, but no staining was seen for the laminin α1, α2, or α3 chains (not shown). No compensatory upregulation of any of these chains was detected in the −/− mice (not shown). Around 10 days

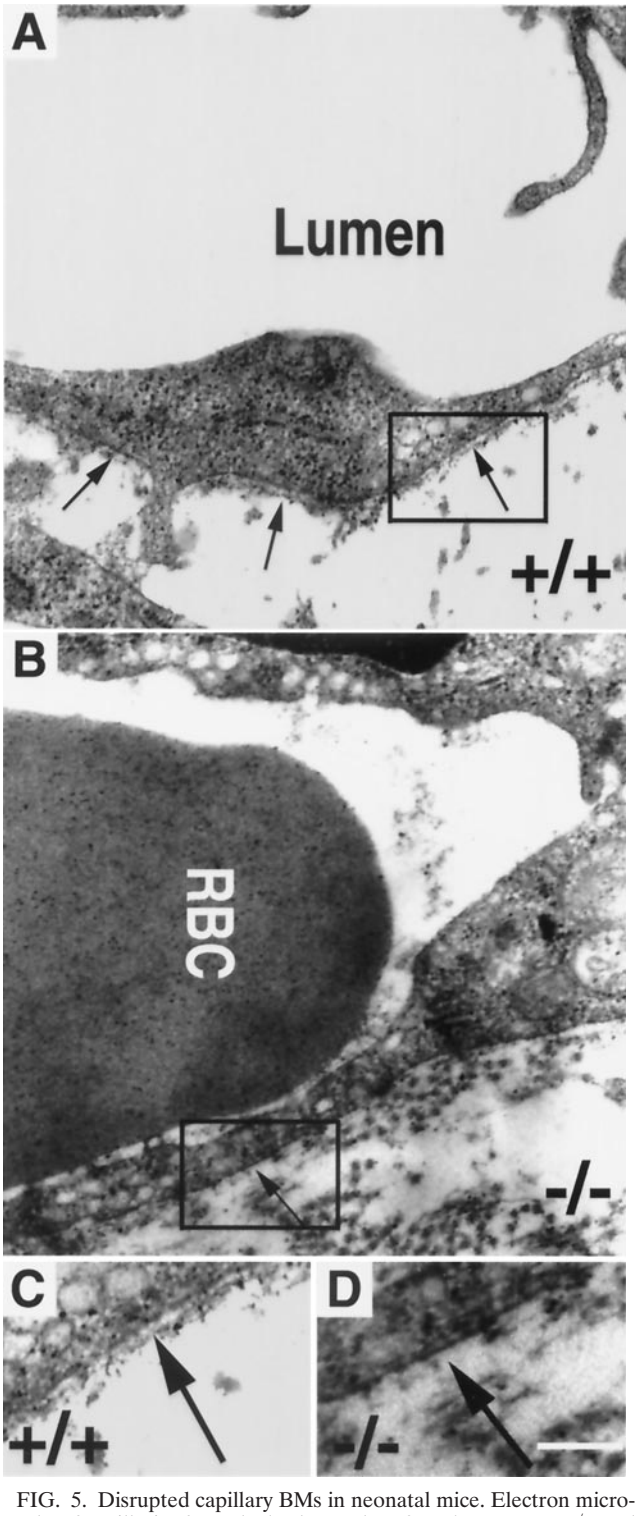

FIG. 5. Disrupted capillary BMs in neonatal mice. Electron micrographs of capillaries from the back muscles of newborn *Lama4*$^{-/-}$ and *Lama4*$^{+/+}$ pups. The capillary BM in control mice is seen as a continuous structure, with a linear lamina densa indicated by arrows (A and C). In mutant mice, the BM is sparser (B) and discontinuous (D; arrow indicates area where BM would have been expected to be). Enlargements (C and D) of the endothelial cell plasma membrane with the adjacent basement membrane are from areas indicated by boxes in panels A and B. An erythrocyte (RBC) is seen in the lumen of the −/− vessel. Bar, 300 nm (A and B) or 150 nm (C and D).

after implantation of the FGF-2 pellet, the swelling was reduced in the null mice, and the blood vessel structure returned to normal (Fig. 6G and H).

DISCUSSION

Analysis of the *Lama4*-null mice generated in this study revealed a central role for laminin-8 (α4:β1:γ1) in microvessel formation. The absence of laminin α4 clearly weakens the capillary BM, with consequent ruptures of the microvascular walls causing hemorrhages, as demonstrated by the bleeding throughout embryonic development. Hemorrhages were seen in −/− embryos already at E11.5, but were most apparent in newborn −/− mice, possibly aggravated by the physical stress of parturition. This notion was further supported by the observation that embryos just prior to birth (E18.5) displayed milder hemorrhages than newborn pups and that the hemorrhages were concentrated in the soft tissues of the head and lower back, which are areas subjected to significant mechanical stress during delivery. Anemia and hemorrhages were found in all newborn −/− animals regardless of genetic background, while they were never seen in heterozygote or wild-type littermates. We surmise the hemorrhages to be the cause of the anemia, which in turn may account for the slightly elevated mortality of null newborns. Blood parameters in the newborn animals indicating sufficient formation of normal erythrocytes were consistent with anemia caused by hemorrhages. Since laminin-8 has recently been found in thrombocytes (7), we wanted to investigate whether the observed hemorrhages could be caused by defective coagulation. However, the bleeding time, which is one test of thrombocyte function, was not prolonged in adult −/− mice, making this hypothesis less likely. Other blood coagulation parameters were also normal.

Immunohistochemical analyses of the newborn null mice indicated that the loss of laminin α4 leads to concomitant loss of β1 and γ1 chains in the muscle capillary BMs. This is not surprising, because an α chain is required for the secretion of laminin β1 and γ1 chains (20, 49), and none of the known laminin α chains were detected in the capillary BMs of the newborn *Lama4*-null mice. However, the loss of laminin α4 was also accompanied by drastic reduction of type IV collagen and nidogen in the capillary BMs of *Lama4*-null mice, whereas the BM-specific proteoglycan perlecan was deposited normally. Defective type IV collagen deposition could explain the structural disorganization of capillary BMs in newborn null mice, as revealed by electron microscopy. The reason for the reduction in type IV collagen and nidogen is not known, but the results suggest that laminin-8 is required for organized assembly of type IV collagen and nidogen into the capillary BM.

There is prior genetic evidence suggesting that laminin is required for BM assembly. Embryos and embryoid bodies devoid of laminin, due to inactivation of the γ1 chain gene, do not form proper BMs (41). In cultured cells, inactivation of laminin synthesis by an antisense strategy also leads to failure of BM formation (5). This concept is also supported by earlier findings in the preimplantation mouse embryo, where laminin appears before type IV collagen (24). Laminin-8 has been shown to bind α6β1 and α6β4 integrins that are typically found on endothelial cells (7, 20). Therefore, it is possible that laminin-8

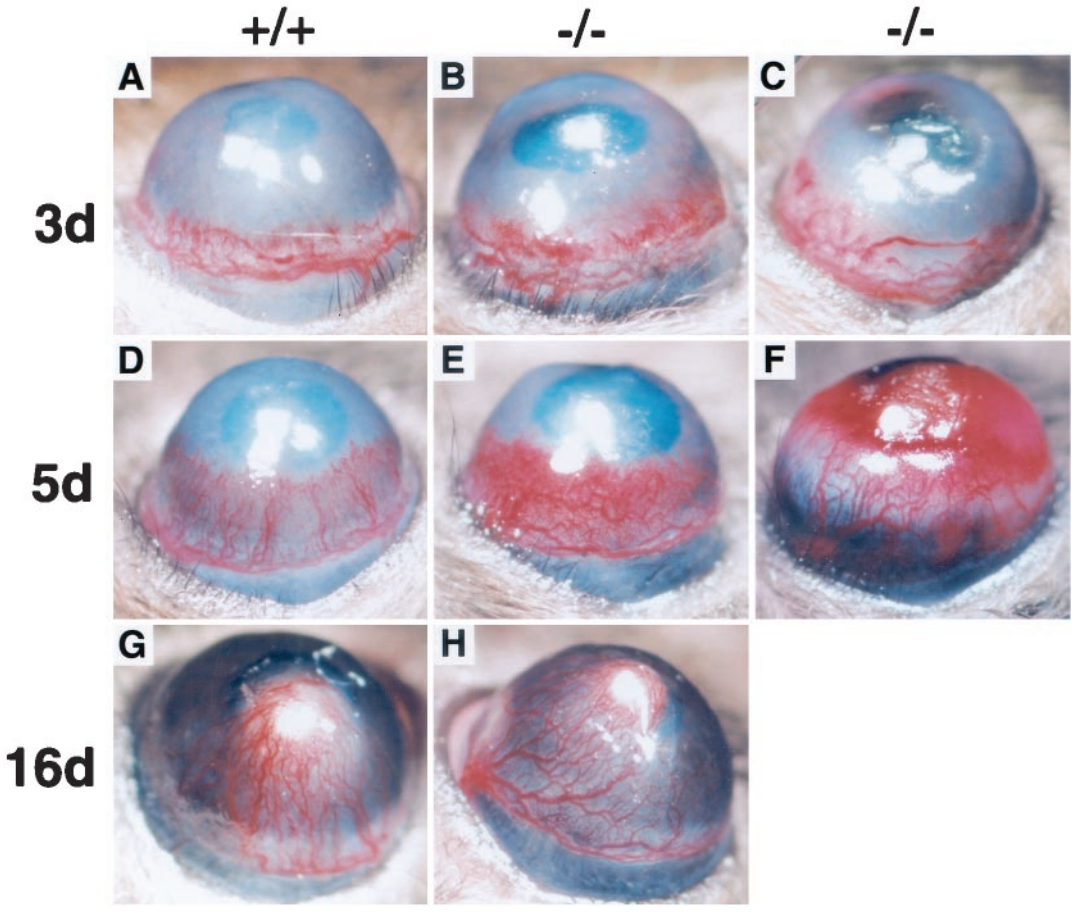

FIG. 6. Cornea angiogenesis assay. In *Lama4*$^{-/-}$ mice, dilated and leaky capillaries could be seen 3 days (3d) after implantation of the FGF-2 pellet (B and C), compared to the findings in wild-type mice at the same time point (A). At 5 days, the distorted growth pattern of the −/− vessels is apparent (E), compared to the pattern in controls (D). The hemorrhages were so severe in about half of the cases, that the animals had to be sacrificed at this time point (F). In the milder cases, the vessels became more stable after 10 days and remained so for up to 16 days (H). The wild-type control after 16 days is shown for comparison (G).

in capillary BMs is bound to the integrins on one the hand and type IV collagen via nidogen on the other. This, in turn, may provide the link between endothelial cell surface and collagen type IV molecules that is essential for the nucleation of the type IV collagen assembly. Alternatively, laminin-8 may function as a signaling molecule, necessary for inducing expression of other BM components. The fact that the vascular phenotype in null mice disappeared during the first weeks of life could be explained by the initiation of expression and deposition of laminin-10 ($\alpha5{:}\beta1{:}\gamma1$) into the capillary BMs during normal early postnatal development, where it is retained (normally together with laminin-8) into adulthood (43). The presence of laminin-10 could facilitate type IV collagen and nidogen deposition, thus restoring BM stability. The type IV collagen and nidogen staining in BMs of individual muscle cells was not altered in newborn laminin $\alpha4$-null mice. This might be explained by the fact the $\alpha2$ and $\alpha5$ chains are expressed in this location at this developmental stage in addition to $\alpha4$ (31).

The crucial role of laminin-8 in the formation of new capillaries was clearly demonstrated in the cornea angiogenesis assay carried out with *Lama4*-null mice, where FGF-2 was used to induce the formation of new blood vessels in the normally avascular cornea. In these experiments, more than half of the mice had to be sacrificed due to extensive hemorrhages and swelling of the cornea. However, similarly to the microvessels in newborn null mice, these vessels eventually assumed an apparently normal structure with time. Our data support other findings demonstrating the important role of BM formation for the angiogenesis process: For example, it has recently been shown that angiogenesis can be drastically decreased in several experimental angiogenesis assays by targeted intervention of type IV collagen assembly (32).

At this moment, one can only speculate on the role of laminin-8 in proper vessel formation. It is possible that the absence of laminin-8 leads to an imbalance between factors promoting vessel maturation and factors that promote endothelial cell migration and proliferation. This, in turn, could lead to excessive and unstable vessel formation in the cornea of the −/− mice. Laminin-8 deposited by the endothelial cells could also be of importance for the recruitment of pericytes, which have been shown to be important for vessel stability (26). Gene targeting experiments have shown that numerous molecules are involved in the complex process of blood vessel formation, including growth factors such as vascular endothelial growth

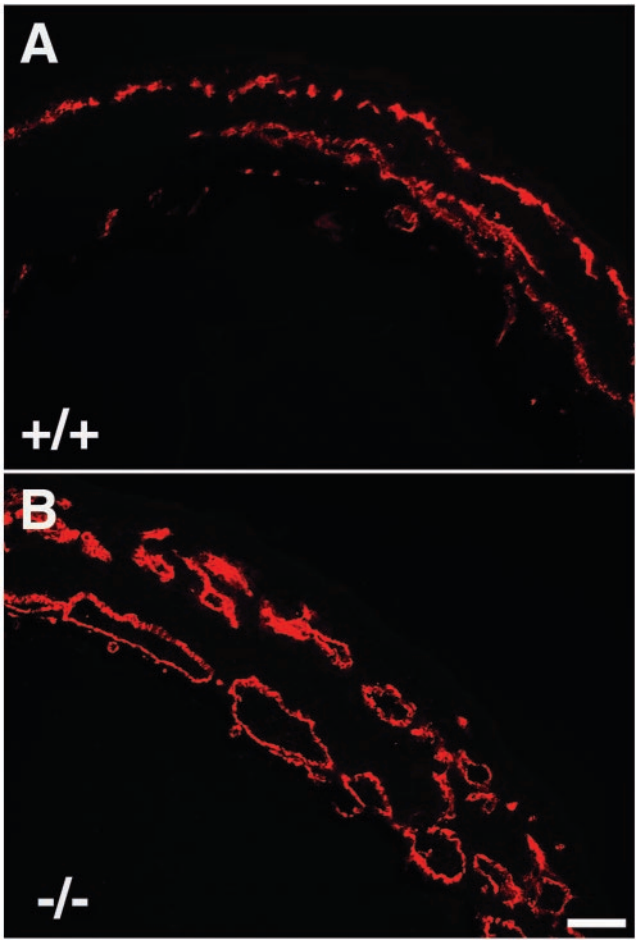

FIG. 7. Dilated newly formed vessels in the cornea angiogenesis assay. Cross-sectioned cornea, 4 days after implantation of the FGF-2 pellet, stained with an antibody against the endothelial cell marker PECAM-1. The vessels in the *Lama4*$^{-/-}$ mice were grossly dilated (B) compared to those in the wild type (A). Bar, 100 μm.

factor, FGF-2, platelet-derived growth factor (PDGF), and the angiopoetins, the receptors of these molecules, as well as cell adhesion molecules (e.g., integrins). Many of the resulting phenotypes show severe defects in angiogenesis during development and a high rate of embryonic lethality (for review, see references 1 and 11). In contrast, *Lama4*-null mice exhibited normal angiogenesis, while only the stability of newly formed vessels was compromised. Defects in vessel stability have been found in PDGF-B-deficient mice, which show fatal hemorrhages prior to birth (25). These mice exhibit microvascular defects such as microaneurysms, possibly due to lack of pericytes (26). Recently, the inactivation of the gene encoding the extracellular matrix protein fibulin-1 was shown to generate changes similar to those in *Lama4*-null mice (21). In fibulin-1-deficient mice, the hemorrhages start during embryonic development, but they are more severe and lead to a high degree of prenatal mortality. Embryos surviving to term show hemorrhages in similar locations, such as in soft tissues of the head and hind limbs, as in *Lama4*-null mice. Another striking observation is that some fibulin-1-deficient mice survived in spite of severe perinatal hemorrhages and cleared all signs of bleeding during the first few days of life. This was also the case with the *Lama4*-null mice, although the hemorrhages were much less severe. The mechanisms underlying vessel instability in *Lama4*-null mice and fibulin-1-deficient mice also seem to differ, since the latter displayed endothelial cell abnormalities, but normal endothelial cell BMs.

In conclusion, absence of the laminin α4 chain leads to defective BMs of capillaries. In addition, the mice have a nonprogressive impairment of locomotion, which could be related to abnormalities in the neuromuscular junction (30). Since the hitherto known inherited laminin diseases (i.e., junctional epidermolysis bullosa and congenital muscular dystrophy [12, 18, 35, 36, 47]) have corresponding disorders in mice (22, 38, 48), the phenotype observed in *Lama4*$^{-/-}$ mice is likely to have a human disease counterpart. However, to date, such a disease has not been identified.

ACKNOWLEDGMENTS

We thank Petra Granquist, Maria Laisi, Johanna Isopahkala, Johanna Räisänen, Ulla Mikkonen, and Wanda Ternström for technical assistance; Mats Estonius, Bernt Jones, and Lars-Olof Hansson for assistance with blood analysis; and Manuel Patarroyo and Maureen Ryan for antibodies. We also thank Ulrich Bergmann and Timo Pikkarainen for critical reading of the manuscript.

This work was supported in part by grants from the Novo Nordisk Foundation, the Swedish Medical Research Council, The Swedish Cancer Foundation, EU grant no. QLGI-CT-01131, and the Human Frontier Science Program.

Jill Thyboll and Jarkko Kortesmaa contributed equally to this work.

REFERENCES

1. **Beck, L., Jr., and P. A. D'Amore.** 1997. Vascular development: cellular and molecular regulation. FASEB J. **11:**365–373.
2. **Cao, Y., and R. Cao.** 1999. Angiogenesis inhibited by drinking tea. Nature **398:**381.
3. **Cao, Y., P. Linden, J. Farnebo, R. Cao, A. Eriksson, V. Kumar, J. H. Qi, L. Claesson-Welsh, and K. Alitalo.** 1998. Vascular endothelial growth factor C induces angiogenesis in vivo. Proc. Natl. Acad. Sci. USA **95:**14389–14394.
4. **Colognato, H., and P. D. Yurchenco.** 2000. Form and function: the laminin family of heterotrimers. Dev. Dyn. **218:**213–234.
5. **De Arcangelis, A., P. Neuville, R. Boukamel, O. Lefebvre, M. Kedinger, and P. Simon-Assmann.** 1996. Inhibition of laminin alpha 1-chain expression leads to alteration of basement membrane assembly and cell differentiation. J. Cell Biol. **133:**417–430.
6. **Frieser, M., H. Nockel, F. Pausch, C. Roder, A. Hahn, R. Deutzmann, and L. M. Sorokin.** 1997. Cloning of the mouse laminin alpha 4 cDNA. Expression in a subset of endothelium. Eur. J. Biochem. **246:**727–735.
7. **Geberhiwot, T., S. Ingerpuu, C. Pedraza, M. Neira, U. Lehto, I. Virtanen, J. Kortesmaa, K. Tryggvason, E. Engvall, and M. Patarroyo.** 1999. Blood platelets contain and secrete laminin-8 (alpha4beta1gamma1) and adhere to laminin-8 via alpha6beta1 integrin. Exp. Cell. Res. **253:**723–732.
8. **Geberhiwot, T., Z. Wondimu, S. Salo, T. Pikkarainen, J. Kortesmaa, K. Tryggvason, I. Virtanen, and M. Patarroyo.** 2000. Chain specificity assignment of monoclonal antibodies to human laminins by using recombinant laminin beta1 and gamma1 chains. Matrix Biol. **19:**163–167.
9. **Gerl, M., K. Mann, M. Aumailley, and R. Timpl.** 1991. Localization of a major nidogen-binding site to domain III of laminin B2 chain. Eur. J. Biochem. **202:**167–174.
10. **Gil, S. G., T. A. Brown, M. C. Ryan, and W. G. Carter.** 1994. Junctional epidermolysis bullosis: defects in expression of epiligrin/nicein/kalinin and integrin beta 4 that inhibit hemidesmosome formation. J. Investig. Dermatol. **103:**31S–38S.
11. **Hanahan, D.** 1997. Signaling vascular morphogenesis and maintenance. Science **277:**48–50.
12. **Helbling-Leclerc, A., X. Zhang, H. Topaloglu, C. Cruaud, F. Tesson, J. Weissenbach, F. M. Tome, K. Schwartz, M. Fardeau, K. Tryggvason et al.** 1995. Mutations in the laminin alpha 2-chain gene (LAMA2) cause merosin-deficient congenital muscular dystrophy. Nat. Genet. **11:**216–218.
13. **Iivanainen, A., J. Kortesmaa, C. Sahlberg, T. Morita, U. Bergmann, I. Thesleff, and K. Tryggvason.** 1997. Primary structure, developmental expression, and immunolocalization of the murine laminin alpha4 chain. J. Biol. Chem. **272:**27862–27868.
14. **Iivanainen, A., T. Morita, and K. Tryggvason.** 1999. Molecular cloning and

tissue-specific expression of a novel murine laminin gamma3 chain. J. Biol. Chem. **274:**14107–14111.
15. **Iivanainen, A., K. Sainio, H. Sariola, and K. Tryggvason.** 1995. Primary structure and expression of a novel human laminin alpha 4 chain. FEBS Lett. **365:**183–188.
16. **Jucker, M., M. Tian, D. D. Norton, C. Sherman, and J. W. Kusiak.** 1996. Laminin alpha 2 is a component of brain capillary basement membrane: reduced expression in dystrophic dy mice. Neuroscience **71:**1153–1161.
17. **Kenyon, B. M., E. E. Voest, C. C. Chen, E. Flynn, J. Folkman, and R. J. D'Amato.** 1996. A model of angiogenesis in the mouse cornea. Investig. Ophthalmol. Vis. Sci. **37:**1625–1632.
18. **Kivirikko, S., J. A. McGrath, C. Baudoin, D. Aberdam, S. Ciatti, M. G. Dunnill, J. R. McMillan, R. A. Eady, J. P. Ortonne, G. Meneguzzi et al.** 1995. A homozygous nonsense mutation in the alpha 3 chain gene of laminin 5 (LAMA3) in lethal (Herlitz) junctional epidermolysis bullosa. Hum. Mol. Genet. **4:**959–962.
19. **Koch, M., P. F. Olson, A. Albus, W. Jin, D. D. Hunter, W. J. Brunken, R. E. Burgeson, and M. F. Champliaud.** 1999. Characterization and expression of the laminin gamma3 chain: a novel, non-basement membrane-associated, laminin chain. J. Cell Biol. **145:**605–618.
20. **Kortesmaa, J., P. Yurchenco, and K. Tryggvason.** 2000. Recombinant laminin-8 (alpha4:beta1:gamma1). Production, purification, and interactions with integrins. J. Biol. Chem. **275:**14853–14859.
21. **Kostka, G., R. Giltay, W. Bloch, K. Addicks, R. Timpl, R. Fässler, and M. L. Chu.** 2001. Perinatal lethality and endothelial cell abnormalities in several vessel compartments of fibulin-1-deficient mice. Mol. Cell. Biol. **21:**7025–7034.
22. **Kuster, J. E., M. H. Guarnieri, J. G. Ault, L. Flaherty, and P. J. Swiatek.** 1997. IAP insertion in the murine LamB3 gene results in junctional epidermolysis bullosa. Mamm. Genome **8:**673–681.
23. **Lefebvre, O., L. Sorokin, M. Kedinger, and P. Simon-Assmann.** 1999. Developmental expression and cellular origin of the laminin alpha2, alpha4, and alpha5 chains in the intestine. Dev. Biol. **210:**135–150.
24. **Leivo, I., A. Vaheri, R. Timpl, and J. Wartiovaara.** 1980. Appearance and distribution of collagens and laminin in the early mouse embryo. Dev. Biol. **76:**100–114.
25. **Leveen, P., M. Pekny, S. Gebre-Medhin, B. Swolin, E. Larsson, and C. Betsholtz.** 1994. Mice deficient for PDGF B show renal, cardiovascular, and hematological abnormalities. Genes Dev. **8:**1875–1887.
26. **Lindahl, P., B. R. Johansson, P. Leveen, and C. Betsholtz.** 1997. Pericyte loss and microaneurysm formation in PDGF-B-deficient mice. Science **277:**242–245.
27. **Liu, J., and R. Mayne.** 1996. The complete cDNA coding sequence and tissue-specific expression of the mouse laminin alpha 4 chain. Matrix Biol. **15:**433–437.
28. **Miner, J. H., J. Cunningham, and J. R. Sanes.** 1998. Roles for laminin in embryogenesis: exencephaly, syndactyly, and placentopathy in mice lacking the laminin alpha5 chain. J. Cell Biol. **143:**1713–1723.
29. **Miner, J. H., B. L. Patton, S. I. Lentz, D. J. Gilbert, W. D. Snider, N. A. Jenkins, N. G. Copeland, and J. R. Sanes.** 1997. The laminin alpha chains: expression, developmental transitions, and chromosomal locations of alpha1–5, identification of heterotrimeric laminins 8–11, and cloning of a novel alpha3 isoform. J. Cell Biol. **137:**685–701.
30. **Patton, B. L., J. M. Cunningham, J. Thyboll, J. Kortesmaa, H. Westerblad, L. Edstrom, K. Tryggvason, and J. R. Sanes.** 2001. Properly formed but improperly localized synaptic specializations in the absence of laminin alpha4. Nat. Neurosci. **4:**597–604.
31. **Patton, B. L., J. H. Miner, A. Y. Chiu, and J. R. Sanes.** 1997. Distribution and function of laminins in the neuromuscular system of developing, adult, and mutant mice. J. Cell Biol. **139:**1507–1521.
32. **Petitclerc, E., A. Boutaud, A. Prestayko, J. Xu, Y. Sado, Y. Ninomiya, M. P. Sarras, Jr., B. G. Hudson, and P. C. Brooks.** 2000. New functions for non-collagenous domains of human collagen type IV. Novel integrin ligands inhibiting angiogenesis and tumor growth in vivo. J. Biol. Chem. **275:**8051–8061.
33. **Poschl, E., J. W. Fox, D. Block, U. Mayer, and R. Timpl.** 1994. Two noncontiguous regions contribute to nidogen binding to a single EGF-like motif of the laminin gamma 1 chain. EMBO J. **13:**3741–3747.
34. **Powell, S. K., and H. K. Kleinman.** 1997. Neuronal laminins and their cellular receptors. Int. J. Biochem. Cell. Biol. **29:**401–414.
35. **Pulkkinen, L., A. M. Christiano, T. Airenne, H. Haakana, K. Tryggvason, and J. Uitto.** 1994. Mutations in the gamma 2 chain gene (LAMC2) of kalinin/laminin 5 in the junctional forms of epidermolysis bullosa. Nat. Genet. **6:**293–297.
36. **Pulkkinen, L., A. M. Christiano, D. Gerecke, D. W. Wagman, R. E. Burgeson, M. R. Pittelkow, and J. Uitto.** 1994. A homozygous nonsense mutation in the beta 3 chain gene of laminin 5 (LAMB3) in Herlitz junctional epidermolysis bullosa. Genomics **24:**357–360.
37. **Ringelmann, B., C. Roder, R. Hallmann, M. Maley, M. Davies, M. Grounds, and L. Sorokin.** 1999. Expression of laminin alpha1, alpha2, alpha4, and alpha5 chains, fibronectin, and tenascin-C in skeletal muscle of dystrophic 129ReJ dy/dy mice. Exp. Cell. Res. **246:**165–182.
38. **Ryan, M. C., K. Lee, Y. Miyashita, and W. G. Carter.** 1999. Targeted disruption of the LAMA3 gene in mice reveals abnormalities in survival and late stage differentiation of epithelial cells. J. Cell Biol. **145:**1309–1323.
39. **Schuler, F., and L. M. Sorokin.** 1995. Expression of laminin isoforms in mouse myogenic cells in vitro and in vivo. J. Cell Sci. **108:**3795–3805.
40. **Sixt, M., B. Engelhardt, F. Pausch, R. Hallmann, O. Wendler, and L. M. Sorokin.** 2001. Endothelial cell laminin isoforms, laminins 8 and 10, play decisive roles in T cell recruitment across the blood-brain barrier in experimental autoimmune encephalomyelitis. J. Cell Biol. **153:**933–946.
41. **Smyth, N., H. S. Vatansever, P. Murray, M. Meyer, C. Frie, M. Paulsson, and D. Edgar.** 1999. Absence of basement membranes after targeting the LAMC1 gene results in embryonic lethality due to failure of endoderm differentiation. J. Cell Biol. **144:**151–160.
42. **Sorokin, L. M., S. Conzelmann, P. Ekblom, C. Battaglia, M. Aumailley, and R. Timpl.** 1992. Monoclonal antibodies against laminin A chain fragment E3 and their effects on binding to cells and proteoglycan and on kidney development. Exp. Cell. Res. **201:**137–144.
43. **Sorokin, L. M., F. Pausch, M. Frieser, S. Kroger, E. Ohage, and R. Deutzmann.** 1997. Developmental regulation of the laminin alpha5 chain suggests a role in epithelial and endothelial cell maturation. Dev. Biol. **189:**285–300.
44. **Talts, J. F., T. Sasaki, N. Miosge, W. Gohring, K. Mann, R. Mayne, and R. Timpl.** 2000. Structural and functional analysis of the recombinant G domain of the laminin alpha4 chain and its proteolytic processing in tissues. J. Biol. Chem. **275:**35192–35199.
45. **Tian, M., C. Jacobson, S. H. Gee, K. P. Campbell, S. Carbonetto, and M. Jucker.** 1996. Dystroglycan in the cerebellum is a laminin alpha 2-chain binding protein at the glial-vascular interface and is expressed in Purkinje cells. Eur. J. Neurosci. **8:**2739–2747.
46. **Timpl, R., and J. C. Brown.** 1996. Supramolecular assembly of basement membranes. Bioessays **18:**123–132.
47. **Tome, F. M., T. Evangelista, A. Leclerc, Y. Sunada, E. Manole, B. Estournet, A. Barois, K. P. Campbell, and M. Fardeau.** 1994. Congenital muscular dystrophy with merosin deficiency. C. R. Acad. Sci. Ser. III **317:**351–357.
48. **Xu, H., X. R. Wu, U. M. Wewer, and E. Engvall.** 1994. Murine muscular dystrophy caused by a mutation in the laminin alpha 2 (Lama2) gene. Nat. Genet. **8:**297–302.
49. **Yurchenco, P. D., Y. Quan, H. Colognato, T. Mathus, D. Harrison, Y. Yamada, and J. J. O'Rear.** 1997. The alpha chain of laminin-1 is independently secreted and drives secretion of its beta- and gamma-chain partners. Proc. Natl. Acad. Sci. USA **94:**10189–10194.